Academic Journal of Nawroz University (AJNU), Vol.11, No.3, 2022

https://doi.org/10.25007/ajnu.v11n3a1423

# The Effect of the First and Second Stress Invariants (Hydrostatic and Deviatoric Stresses) on the Compressibility Function

Abdulamir Sahm Resen
Department Computer Engineering and Communication, Nawroz University, Duhok, KRG - Iraq

## ABSTRACT

Experimental work was carried out to investigate the separate roles of the hydrostatic and deviatoric components of stress tensor (Using the First and the second invariants $I_1$ and $I_2'$). The results were expressed in term of stress dependent shear compliance J and apparent compressibility function B in the time temperature region of the test (up to $10^4$ seconds at 30℃ the region of the $\alpha$ −relaxation).

The Compressibility Function B showed no significant change, when increasing the hydrostatic stress $I_1$ and keeping the deviatoric stress $I_2'$ constant, and by varying $I_2'$ and keeping $I_1$ constant the change is about 10% for the stress combination of tension-torsion.

The volume was found to increase with time when increasing $I_2'$ and keeping $I_1$ constant.

In the case of J and B the deviatoric stress $I_2'$ played the major role. All these effects could be rationalized by the idea of the time dependent free volume. If the free - volume increases with time by increasing $I_2'$ this could explain the difference in the effect of $I_1$ and $I_2'$ on B and explain the creep less than recovery.

There is no difference between the compressibility function in creep and recovery (to within the experimental scatter of (12%)).

A small increase in B was detected with time, the maximum difference between the lowest and highest B is 5.9%.

**Keywords**: *Stress, Hydrostatic Stress, Deviatoric Stress.*

### 1. Introduction

Uniaxial and biaxial creep and recovery experiments were carried out on tubular specimens of isotropic PMMA to investigate the separate roles of the hydrostatic and deviatoric components of stress. These experiments were carried out using different stress combinations (tension-torsion) varying the first and second stress invariants $I_1$ and $I_2'$ and extending the measurements to the non-linear region [1].

The three strains $e_1$, $e_2$, and $\gamma$ were needed in order to find the shear compliance J , acompressibility function B. These strains were measured directly, therefor there is no need for any assumption. The theory of linear viscoelastic solids extended to take into the account the non-linear region. For creep experiment in which the stress tensor $\sigma$ is applied at time equal to zero, defined by the mean stress $\sigma_m$, and the deviatoric stress tensor $\sigma'$ [2].

$$\sigma_m = 1/3\ \mathrm{tr}\sigma \qquad (1.1)$$

$$\underset{\sim}{\sigma'} = \underset{\sim}{\sigma} - \underset{\sim}{I}\,\sigma_m$$

$$\sigma_m = (\sigma_{11} + \sigma_{22} + \sigma_{33})/3 \qquad (1.2)$$

From equation (1.1) the deviatoric stress tensor

$$\underset{\sim}{\sigma'} = \begin{bmatrix} (\sigma_{11} - \sigma_m) & \sigma_{12} & \sigma_{13} \\ \sigma_{21} & (\sigma_{22} - \sigma_m) & \sigma_{23} \\ \sigma_{31} & \sigma_{32} & (\sigma_{33} - \sigma_m) \end{bmatrix} \qquad (1.3)$$

From equation (1.2) $\sigma_m = (\sigma_{11})/3$ (1.4)

Where $\sigma_{22} = \sigma_{33} = 0$

From equations (1.2) and (1.3) the deviatoric stress for combined tension-torsion

$$\underset{\sim}{\sigma'} = \begin{bmatrix} (2/3\,\sigma) & \tau & 0 \\ \tau & (-1/3\,\sigma) & 0 \\ 0 & \sigma_{32} & (-1/3\,\sigma) \end{bmatrix}$$

For an isotropic linear viscoelastic solid with the shear compliance function J(t) and the compressibility function B(t), the deformation at $t > 0$ with the strain tensor e(t) equation (1.5) is

$$\underset{\sim}{e}(t) = \frac{J(t)}{2}\underset{\sim}{\sigma'} + \frac{B(t)}{3}\sigma_m \underset{\sim}{I} \qquad (1.5)$$

For non-linear viscoelastic solid whose non-linearity is caused only by J(t) and B(t). This is depended upon the dominating stress state which is defined by its invariants $I_1$, $I_2$, and $I_3$ equation (1.6) where

$$I_1 = \sigma_{11} + \sigma_{22} + \sigma_{33}$$

$$I_2 = -(\sigma_{22}\sigma_{33} + \sigma_{11}\sigma_{33} + \sigma_{11}\sigma_{22}) + \tau_{12}{}^2 + +\tau_{13}{}^2 + \tau_{23}{}^2$$

$$I_3 = (\sigma_{11}\sigma_{22}\sigma_{33} + \sigma_{11}\sigma_{33} + 2\tau_{12}\tau_{23}\tau_{31} - \sigma_{22}\tau_{13}{}^2 - \sigma_{33}\tau_{12}{}^2 \qquad (1.6)$$

It is convenient to work with the first and second stress invariant $I_1$ and $I_2{}'$.
$I_1$ and $I_2{}'$ were chosen to describe the two-dimensional stress response because they are independently separate the hydrostatic and deviatoric stresses.

$I_2{}'$ is analogue to $I_2$ for deviatoric stress $\underset{\sim}{\sigma}'$.

Where for tension-torsion

$$(\sigma_{22} = \sigma_{33} = 0,\ \sigma_{23} = \sigma_{32} = 0,\ \sigma_{13} = \sigma_{31} = 0$$

Assuming that the non-linear case for multiaxial creep response equation should then be

$$\underset{\sim}{e}(t) = [J(t, I_1, I_2, I_3)/2]\underset{\sim}{\sigma}' + [B(t, I_1, I_2, I_3)/3]\sigma_m \underset{\sim}{I} \qquad (1.7)$$

A similar equation has been suggested by Sternstein and Ho [3] for stress relaxation of non-linear viscoelastic solids.
From the above in biaxial tension-torsion, the creep can be determined as follows:
Tensile strain equation (1.8)

$$e_{11} = [J(t, I_1, I_2, I_3)/3] + [B(t, I_1, I_2, I_3)/9]\ \sigma_{11} \qquad (1.8)$$

Shear strain equation (1.9)

$$e_{12} = J(t, I_1, I_2, 0)\ \sigma_{12} \qquad (1.9)$$

Mallon and Banham [4] showed that B(t) (when $I_2{}' = 0$) is independent of $I_1$. Buckley and McCrum [5] suggested that B(t) is also independent of $I_2{}'$.
The lateral contraction equation (1.10) is

$$e_{22} = [-J(t, I_1, I_2, I_3)/3] + [B(t, I_1, I_2, I_3)/9]\sigma \qquad (1.10)$$

Read and Dean [6] measured the tensile and lateral strains. The results showed that apparent tensile compliance increase with increasing tensile load and time. The lateral contraction ratio appears to be constant for the first 150 seconds and after that to increase with increasing load and time. After an increase with time $10^{2.5}$ seconds subsequently the variations in volume strain were small. The apparent compressibility function B(t) was found to occur a little with stress and decrease with time. Passion's ratio was found to be 0.37 ($\text{at } t = 100\text{sec.}$).

It is conventional to use as invariants of three-dimensional stress tensor $\sigma_o$ coefficients in the characteristic equation. [2]

$$I_1 = tr\underset{\sim}{\sigma_o},\quad I_2 = \left[tr\underset{\sim}{\sigma_o}{}^2 - (tr\underset{\sim}{\sigma_o})^2\right],\quad I_3 = det\underset{\sim}{\sigma_o} \qquad (1.11)$$

The stress was composed into a hydrostatic component and deviatoric component $\underset{\sim}{\sigma_o}'$ equation (1.12)

$$\underset{\sim}{\sigma_o}' = \underset{\sim}{\sigma_o} - \frac{1}{3}\underset{\sim}{I}\ tr\underset{\sim}{\sigma_o} \qquad (1.12)$$

To describe the response to two-dimensional proportional loading history the two invariants $I_1$ and $I_2{}'$ were chosen.
Where $I_1 = tr\underset{\sim}{\sigma_o}$, $I_2{}' = \frac{1}{2}\ tr(\underset{\sim}{\sigma_o}')^2$

$I_2{}'$ is analogous to $I_2$, the deviatoric stress $\underset{\sim}{\sigma_o}$ and $\underset{\sim}{\sigma_o}'$ are stress tensors, although $\underset{\sim}{\sigma_o}$ is confined here to a plane stress. $I_1$ and $I_2{}'$ independently characterize the hydrostatic and deviatoric components of the stress.

Consider the response of an isotropic linear viscoelastic material to proportional loading equation (1.13).

$$\underset{\sim}{e}(t) = (J/6 - B/9)I_1\ \underset{\sim}{I} + \frac{J}{2}\ \underset{\sim}{\sigma}' \qquad (1.13)$$

Where $J$ is the shear compliance and $B$ is the compressibility function.

In the case of biaxial tension-torsion on a tubular specimen the stress $\sigma$ and the strain $e$ can be written with respect to the axial and lateral axis in the wall of the tubular specimen [2].

$$e = \begin{bmatrix} e_1 & \frac{\gamma}{2} \\ \frac{\gamma}{2} & e_2 \end{bmatrix} \qquad \sigma_o = \begin{bmatrix} \sigma & \tau \\ \tau & \sigma \end{bmatrix} \qquad (1.14)$$

where $e_1$ is the longitudinal strain, $e_2$ is the lateral strain, $\gamma$ is the shear strain $\sigma$ is the tensile stress and $\tau$ is the shear stress.
From equations (1.11) to (1.13) the stress invariants can be written as follows

$$I_1 = \sigma \qquad I_2{}' = (\sigma^2/3) + \tau^2 \qquad (1.15)$$

It has been shown for the plane stress state (e.g., Tension-torsion stress state) equation (1.13) can be applied even in the non-linear case [7], hence in this situation of the Linear strain equation (16) is used

$$e_1(I_1,\ I_2{}', t) = [J(I_1,\ I_2{}', t)/3 + B(I_1,\ I_2{}', t)/9]\sigma \qquad (1.16)$$

The lateral strain equation (1.17) is

$$-e_2(I_1,\ I_2{}', t) = [J(I_1,\ I_2{}', t)/6 - B(I_1,\ I_2{}', t)/9]\sigma \qquad (1.17)$$

and the shear strain equation (1.18) is

$$\gamma(I_1,\ I_2{}', t) = J(I_1,\ I_2{}', t)\ \tau \qquad (1.18)$$

The temperature was kept constant at ($30 \pm 0.2$℃) throughout the tests. This was chosen as the beginning of ($\alpha$) relaxation (primary relaxation) of this material to avoid aging effects and the effect of high temperature on creep of PMMA.

The change in volume was calculated using the passion's ratio $\mu$ and the tensile strain $e_1$ from the experimental results in tension - torsion (eq.1.19)

$$\Delta V = Ve_1(1-2\mu) \quad (1.19)$$

The experimental result showed an increase in $\Delta V$ with time when the first invariant $I_1$ kept constant and varying the second invariant $I_2{}'$ for the time scale $10^4$ seconds.

Peyman Nikaeen, et.al [8] studied the effect of the macro-scale mechanical deformation on the nanostructure of glassy polymers by scrutinizing the changing their nanoscale mechanical response. The measurement of the mechanical properties of the polycarbonate and poly(methyl methacrylate) specimens was done by using Nanoindentation technique, which were subjected to a prior plastic deformation in uniaxial tension. The measurements were focused on the inelastically deformed and unloaded specimens. The results show that the shear activation volume decreases with inelastic deformation.

## 1- Results and Discussion

The Biaxial (tension-torsion) Creep tests were carried out to find the effect of the first invariant $I_1$ and $I_2{}'$, and describe the effect of these invariants on the behavior of the materials.

These experiments were carried out by keeping the first invariant $I_1$ constant and increasing $I_2{}'$. This was done to find the effect of increasing the second invariant $I_2{}'$ on the tensile strain $e_1$ and the lateral strain $e_2$. The results show that with increasing the second invariants $I_2{}'$the tensile and lateral strains were increased, and the effect with the second invariants $I_2{}'$ increases with increasing time [1].

The passion's ratio $\mu$ was found to be constant with changing $I_2{}'$ when the first invariant $I_1$ was small, and increasing with time when the first invariant $I_1$ was larger.

### 2.1 The effect of $I_1$ and $I_2{}'$on the apparent compressibility function ( $B$)

The effect of increasing $I_2{}'$at different constant $I_1$ on the apparent compressibility function $B$ is shown in Figures (2 to 5). These figures show that with increasing of $I_2{}'$, the apparent compressibility function $B$ increases by about 10%. The compressibility function $B$ was found to vary with time and stress but this variation is not systemic. ($B$) was found to fall slightly at higher stress over the time scale as shown in figure (2 and 3), when ($I_1 = 5.477 MN/m^2$) and ($I_2{}' = 300(MN/m^2)^2$).

Figure (6 to 10) were plotted for the apparent compressibility function $B$ versus log time for a constant $I_2{}'$ and varying $I_1$. These figures show no significant change with changing $I_1$ for the experimental time scale of $10^4$ seconds. This is true for all the experimental stress levels used in this work, where $I_2{}'$ changed from ($50\ to\ 300(MN/m^2)^2$), and kept constant at each $I_2{}'$ level with increasing $I_1$. These experiments were carried out on different specimens.

An increasing of $I_2{}'$ was found to enhance the time dependent component of $B$. The compressibility function $B$ was plotted versus log time (Fig.1), for pure tensile load application to the specimen. This shows an increase of $B$ with increasing the tensile load.

### 2.2 The effect of $I_1$ and $I_2{}'$ on the compressibility function $B$ in recovery $B_r$

The difference between the compressibility function $\Delta B$ in creep and recovery was measured using equation 2.1

$$\Delta B = B_r - B_c \quad (2.1)$$

Figures (11 to 14) show that there is no difference (to within the experimental scatter of 12%) between the compressibility function in creep and recovery;
neither in varying $I_2{}'$ and keeping $I_1$constant nor in varying $I_1$ and keeping $I_2{}'$ for all the stress levels used in these tests.

### 2.3 The effect of $I_1$ and $I_2{}'$ on the compressibility fractional recovery $F_B$

The compressibility fractional recovery $F_B$ was measured in a similar way to the shear compliance fractional recover $F_J$ equation (2.2)

$$F_B = \frac{B_{max}(I_1,I_2{}',t) - B(I_1,I_2{}',t)}{B_{max}(I_1,I_2{}',t)} \quad (2.2)$$

Where $B_{max}$ is the maximum apparent compressibility function in creep, and $B$ is the compressibility function in recovery (fig. 15).

The compressibility function fractional recovery $F_B$ versus log reduced time ($t_R$) shown in figures (16 to 19). These curves are for a constant $I_1$ and increased $I_2{}'$. $I_1$ takes the values of ($4.77, 12.247, 17.32 MN/m^2$) , and ($21.213 MN/m^2$), and $I_2{}'$ increased from ($25\ to\ 300(MN/m^2)^2$). The curves show that $F_B$ is constant (to within the experimental scatter).

Figures (20 to 25) are for $F_B$ at constant $I_2{}'$ and varying $I_1$. The fractional recovery compressibility function $F_B$ is constant with increasing $I_1$ for the experimental time.

The effect of non-linearity could be due to $I_1$ at the beginning of the experimental time, where the effect was due to $I_2{}'$ at a later time. This means that $I_1$ affect the volume at short time and $I_2{}'$ at long time, applying this to the fractional recovery hypotheses it shows that $I_2{}'$ increases the time dependent component of the volume. This is entirely constant with the effect of $I_2{}'$ on the compressibility function $B$ ($I_2{}'$ increasing the time dependent of $B$). Applying this effect to the free volume, shows that $I_2{}'$ increasing the time dependent component of the volume where as $I_1$ simply affect the magnitude of the volume. $I_2{}'$ increases the time dependent of $B$.

The increase of the tensile stress shows an increase in the compressibility function $B$ (Fig. 1). The compressibility function $B$ at constant tensile stress ($I_1$ is constant) and varying $I_2{}'$ show a small increase with time. This increase drops down at the end of the experimental time (Fig. 2 to 5). The measurement of B is subjected to experimental scatter of 18.6%. The difference between the lowest and highest values is 18.2% . Measurement pf PMMA was also done by Read and Dean [6] . They found an increase in $B$ with an increase in the tensile stress, and after $10^4$ seconds $B$ start to increase as the time increased. The dependent of $B$ on the tensile stress and time has an important meaning for the possible structural change and mechanical aging effects generated by applied stress. Read and Dean [6] attribute the increase of the volume to the hydrostatic component of the stress, when a tensile stress in a linear range was applied to a polymer for a short time compared with $\alpha - retardation$ time.

Increasing $I_2{}'$ and keeping $I_1$ constant (Fig. 2 to 5) shows that the increase of $I_2{}'$ increase the compressibility function B by 21% (Fig. 2). A small increase in B was detected with time, the maximum difference between the lowest and highest B is 5.9% .

The increase of $I_1$ and keeping $I_2{}'$ constant shows insignificant change in $B$ (Fig. 6 to 10). The increase of $B$ for anew specimen was mor than would be expected from increasing the stress only (Fig. 1 to 5).

Figures (11 to 14) shows no significant difference (to within the experimental scatter) between the compressibility function and recovery compliance $B\ and\ B_r$ equation (2.3)

$$B_r - B = 0 \qquad (2.3)$$

A similar increase was not detected when torque was applied to the specimens to increase $I_2{}'$ while keeping $I_1$ constant at $8.66 MN/m^2$, passion's ratio $\mu$ seems to be constant under this stress level for the experimental period of time.

**2.4 Volume change**

To measure the change of the compressibility function in terms of $I_1$, and $I_2{}'$, the important factor in this measure is the volume change which can be measured from the pure tensile load application and the dilation where $e_2 = e_3$.

From the results of the shear compliance $J$ and the compressibility function $B$ one can predict the strains from equation (2.4) [2].

$$e(t) = \{[B(I_1, I_2{}', t)/9] - [J(I_1, I_2{}', t)/6]\}I_1, I + [J(I_1, I_2{}', t)/2]\sigma \qquad (2.4)$$

The change of $\Delta V$ at long time is due to the effect of the second invariant $I_2{}'$ (Fig. 26 and Fig. 27).

The non-linearity at the beginning of the experimental time could be due to the first invariant $I_1$, where the effect of the second invariant $I_2{}'$ at a later time. This means that $I_1$ affect the volume at short time and $I_2{}'$ at long time [9] .

**2- Conclusion**

The effect of increasing the second invariant $I_2{}'$ at constant first invariant $I_1$ on the apparent compressibility function $B$ was to increase it by about (25%). $B$ was found to increase with time and stress and to fall slightly at a higher time scale of $10^4$ second. With increasing $I_1$ at constant $I_2{}'$, there was no significant variation to within the scatter 12% for time of $10^4$ seconds. Increasing $I_2{}'$ was found to enhance the time dependent component of $B$.

The tow invariants $I_1$, and $I_2{}'$ showed no significant effect on the difference between apparent compressibility function ($\Delta B = B_r - B_c$) in creep and recovery.

The change in the volume $\Delta V$ at long time is attributed to the effect of the second invariant $I_2{}'$.

The first invariant $I_1$ could affect the non-linearity at the beginning of the experimental time, where the effect was due to $I_2{}'$ at a later time. This means that $I_1$ affect the volume at short time and $I_2{}'$ at long time .

The fractional recovery compressibility function $F_B$ is constant (to within the scatter limit) with increasing $I_1$ , and keeping $I_2{}'$ constant for the experimental time, the same results was found when increasing $I_2{}'$ and keeping $I_1$.

**References**

[1] Resen A. S. (England, 1988) Biaxial Creep of Plastics, PhD. Thesis, University of Manchester Inst. of Sci. and Tech.

[2] Buckley C. P. (1987) Multiaxial nonlinear viscoelasticity of solid polymers, Polymer Eng. Sci. Vol. 27, No. 155

[3] Sternstein, S. S. and HO, T. C. (1972) Biaxial stress relaxation in glassy polymers: Polymethylmethacrylate, J. of Appl. Physics, 43, 4370

[4] Mallon, P. J. and Benham, P. P. (1972) Anisotropic mechanical behaviour of polymers J. Plastics and Polymers, 40, 77

[5] Buckley, C. P., McCrum, N. G. (1974. 5.) The relation between linear and non- linear viscoelasticity of PP, J. Mater. Sci., Vol. 9, PP. 2064-2066,

[6] Read B. E., and Dean G. D. (1984) Time-dependent deformation and craze initiation in PMMA: Volume effects, J. Polymer, 25, 1679,

[7] Buckley, C. P. and Green, A. E. (1976) Small deformation of nonlinear viscoelastic tube: Theory and application to Polypropylene, Phil. Trans. Roy. Soc. London, A Math. Phys. Sci. 281, 543.

[8] Peyman Nikaeen A., Aref Samadi-Dooki B., George Z., Voyiadjis B., Pengfei Zhang A. C., William M., Chirdon A., Ahmed Khattab A., (2021) Effect of plastic deformation on the nanomechanical properties of glassy polymers: An experimental study, Mechanics of Materials 159, 103900

[9] Struik, L. C. E. (1977). Physical aging in amorphous polymers and other materials.

**Appendix**

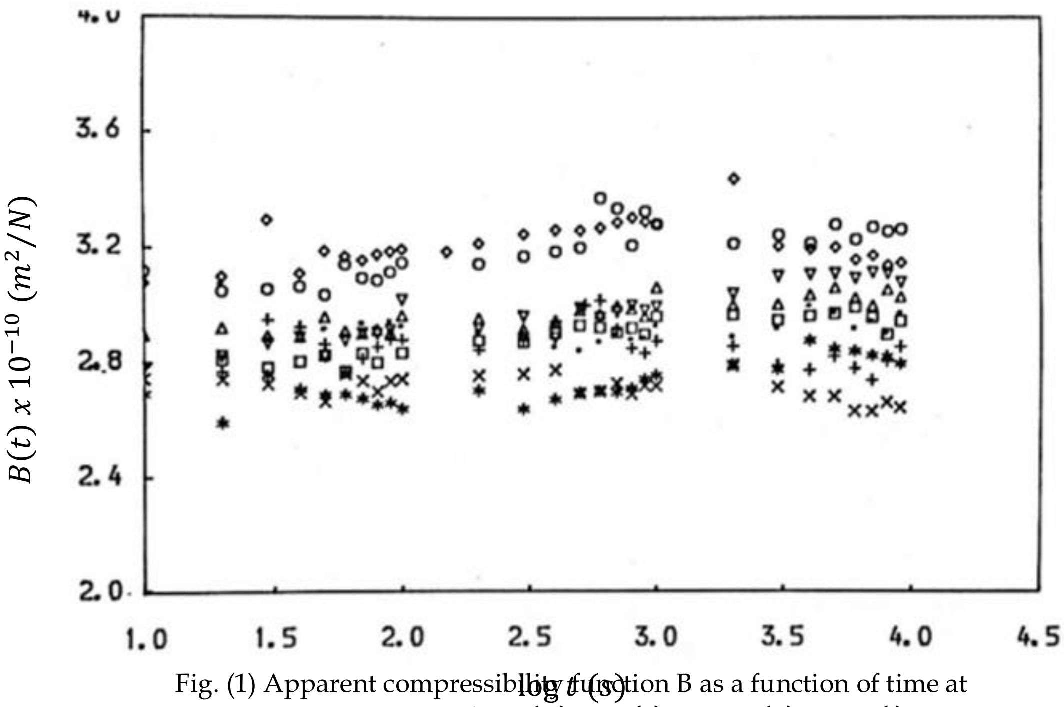


Fig. (1) Apparent compressibility function B as a function of time at constant stress $\sigma = 5.477(+), 8.66(*), 12.247\ (x), 17.32\ (\cdot)$, $21.213(\Delta), 24.2495\ (\nabla), 27.386\ (\square), 30.00(\lozenge), MN/m^2$

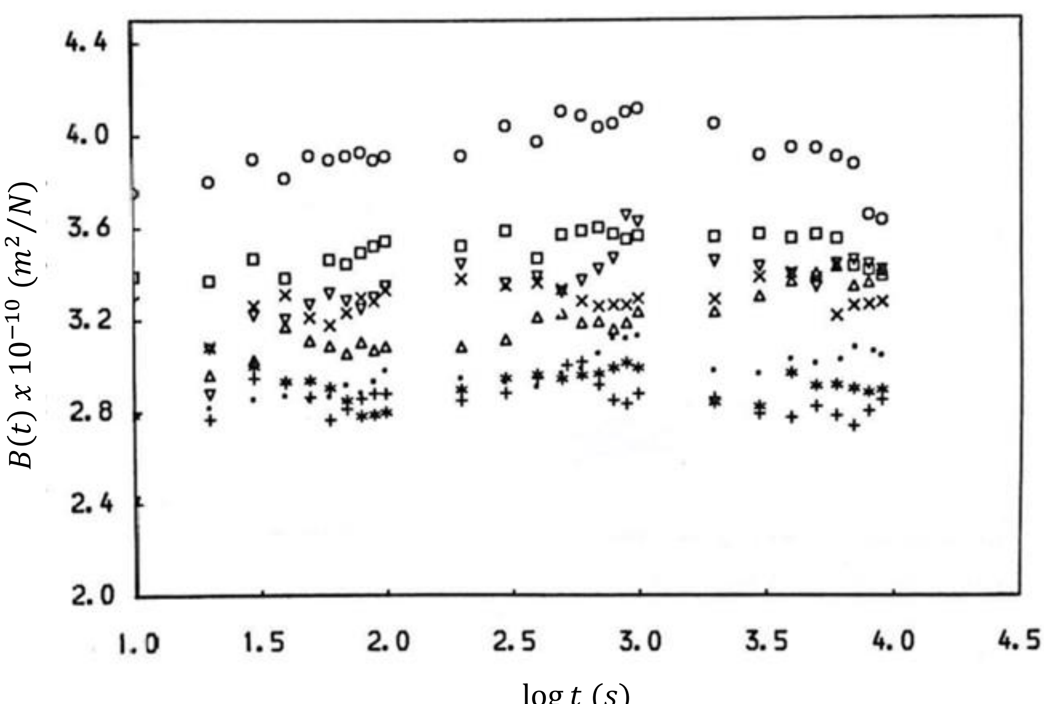


Fig. (2) Apparent compressibility function B as a function of time at constant $I_1 = 5.477MN/m^2, varying\ I_2{}' = 10(+),\ 25(*)$, $50(X), 100(\cdot), 150(\Delta), 200\ (\nabla), 250\ (\square)$,$300\ (\lozenge)$, $(MN/m^2)^2$

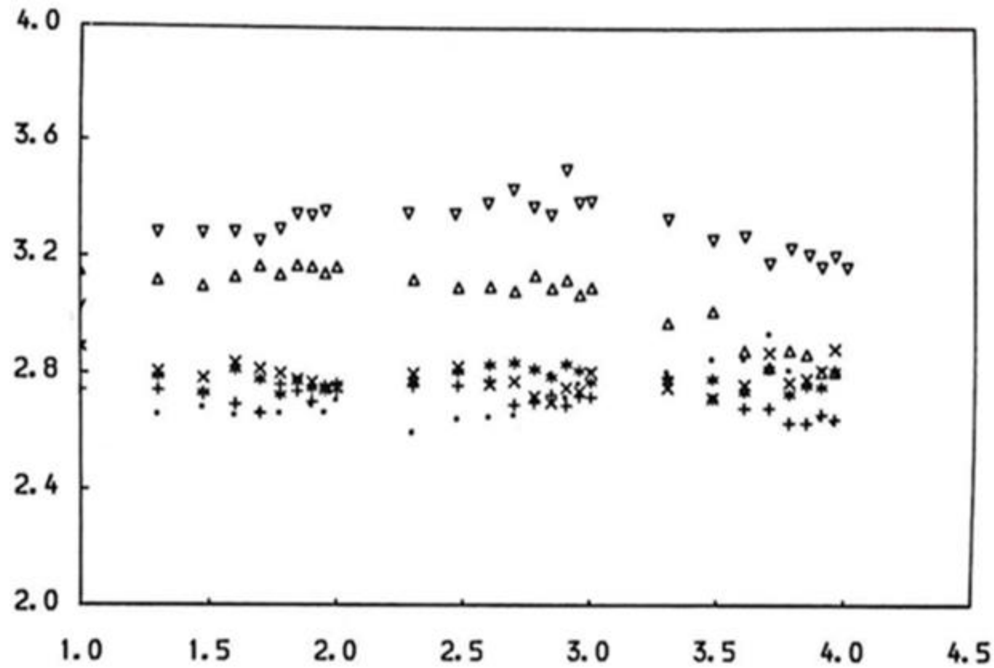


Fig. (3) Apparent compressibility function B as a function of time at constant $I_1 = 12.247 MN/m^2, varying\ I_2{}' = 50(+),\ 100(*),\ 150(X), 200(\cdot), 250(\Delta), 300\ (\nabla)\ (MN/m^2)^2$

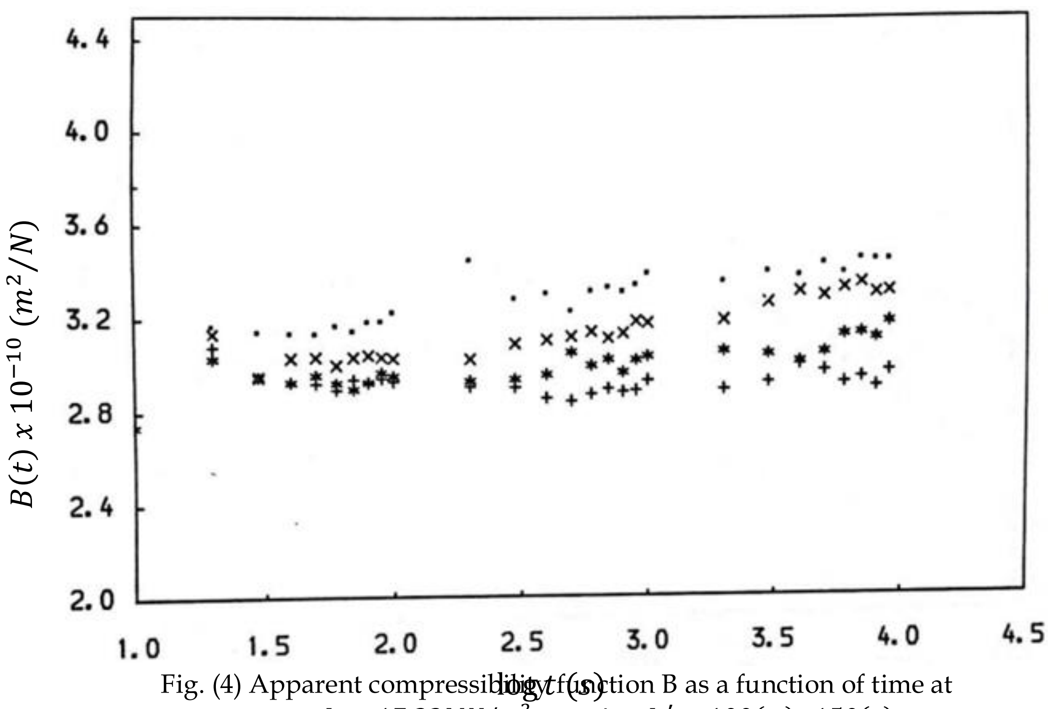


Fig. (4) Apparent compressibility function B as a function of time at constant $I_1 = 17.23 MN/m^2, varying\ I_2{}' = 100(+),\ 150(*),\ 200(X), 250(\cdot), (MN/m^2)^2$

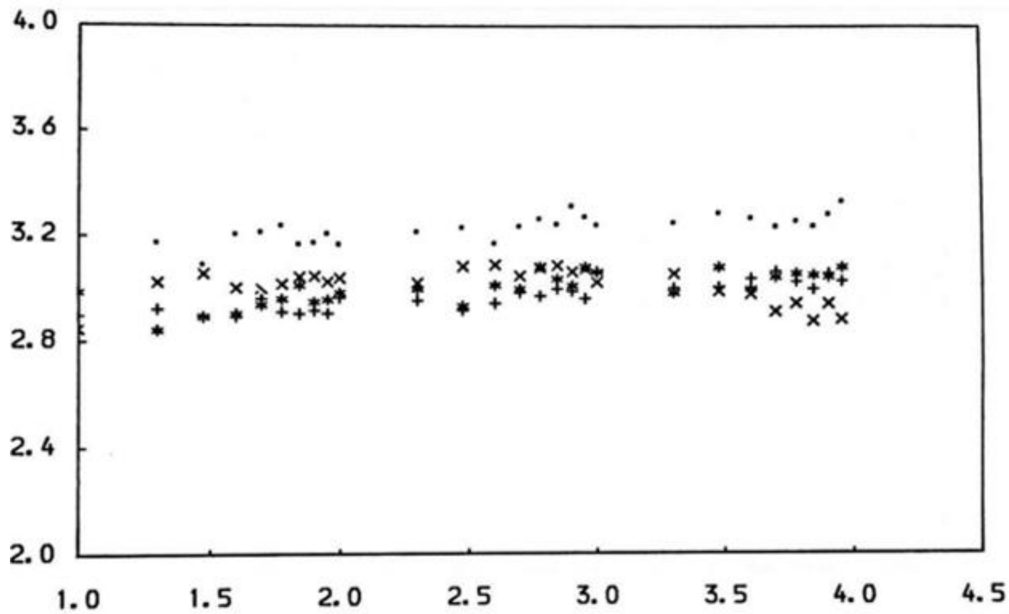


$\log t\,(s)$

Fig. (5) Apparent compressibility function B as a function of time at Constant $I_1 = 21.213\ MN/m^2\ varying\ I_2{}' = 150\ (+), 200\ (*)$, $250\ (X), 300\ (\cdot), (MN/m^2)^{\ 2}$

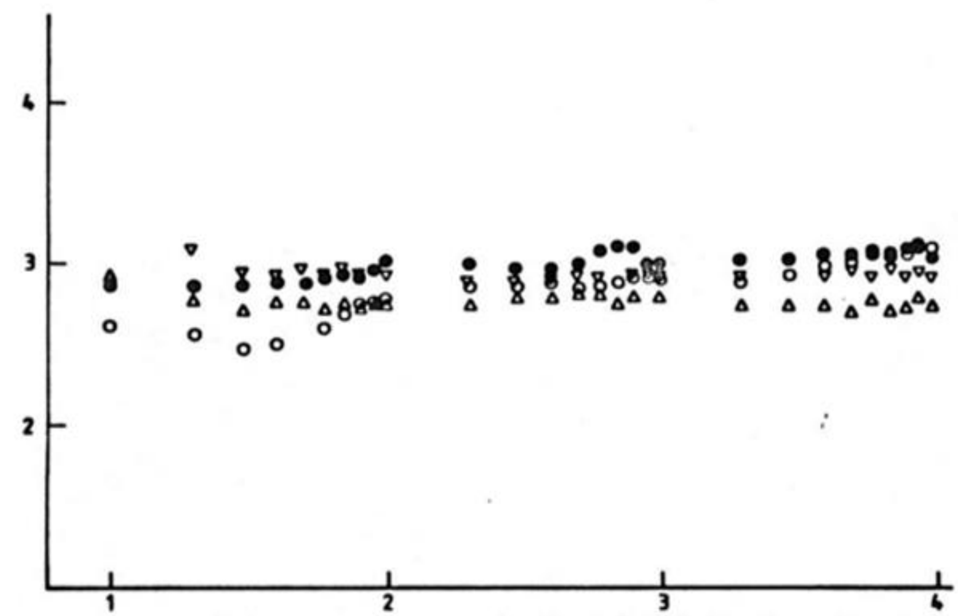


$\log t\,(s)$

Fig. (6) Apparent compressibility function B as a function of time at $I_2{}' = 100\ (MN/m^2)^{\ 2}\ \ varying\ I_1 = 5.477$ (●), 8.66 (◯), 12.247(Δ), 17.32(▽), $MN/m^2$

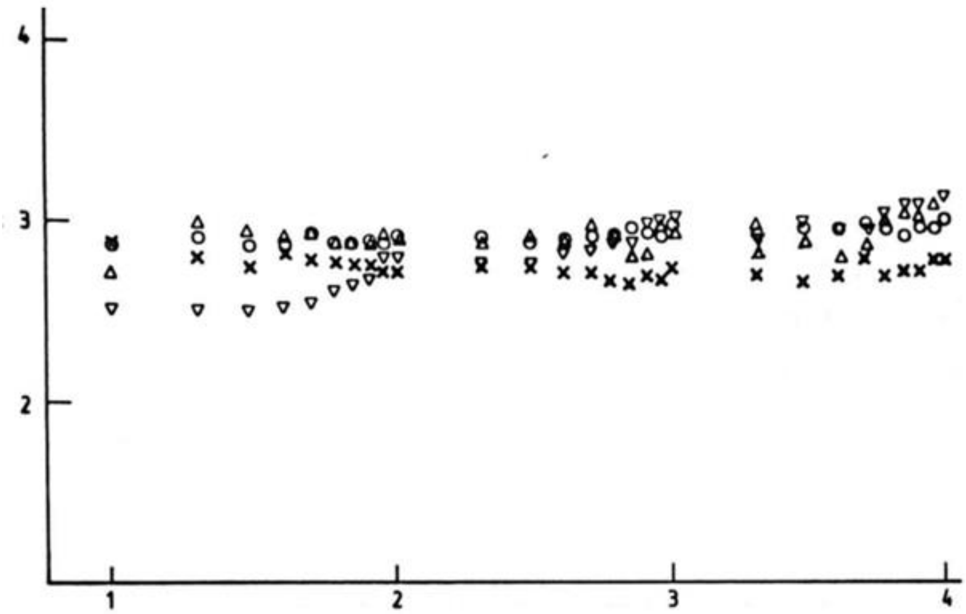


Fig. (7) Apparent compressibility function B as a function of time at constant $I_2' = 150\ (MN/m^2)^2$ $varying\ I_1 = 5.477\ (X)$, $12.247$ (◯), $17.32$(Δ), $21.213$(▽), $MN/m^2$

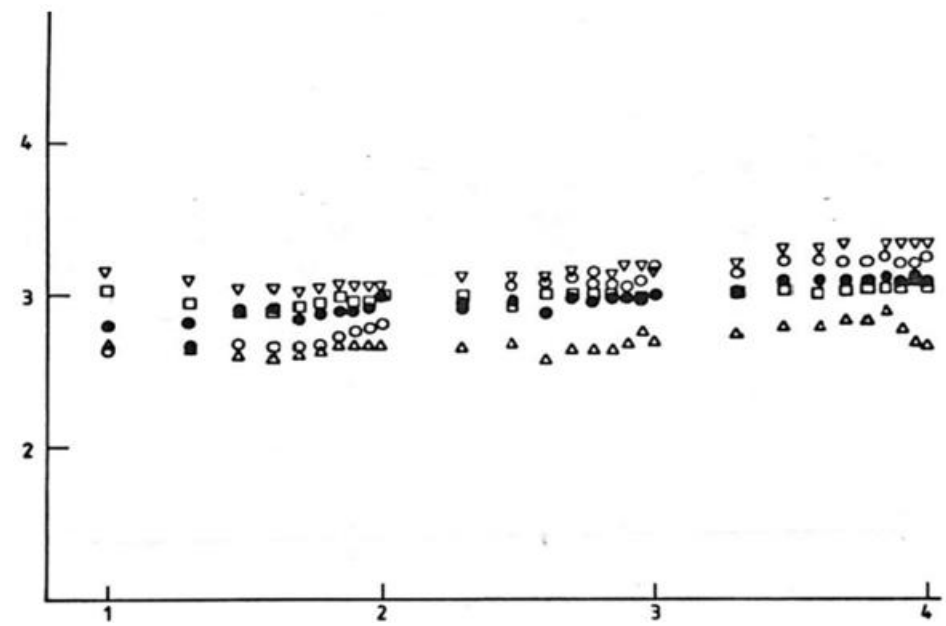


Fig. (8) Apparent compressibility function B as a function of time at constant $I_2' = 200\ (MN/m^2)^2$ $varying\ I_1 = 8.66$ (◯), $12.247$ (Δ), $17.32$(▽), $21.213$(□), $24.495$(●) $MN/m^2$

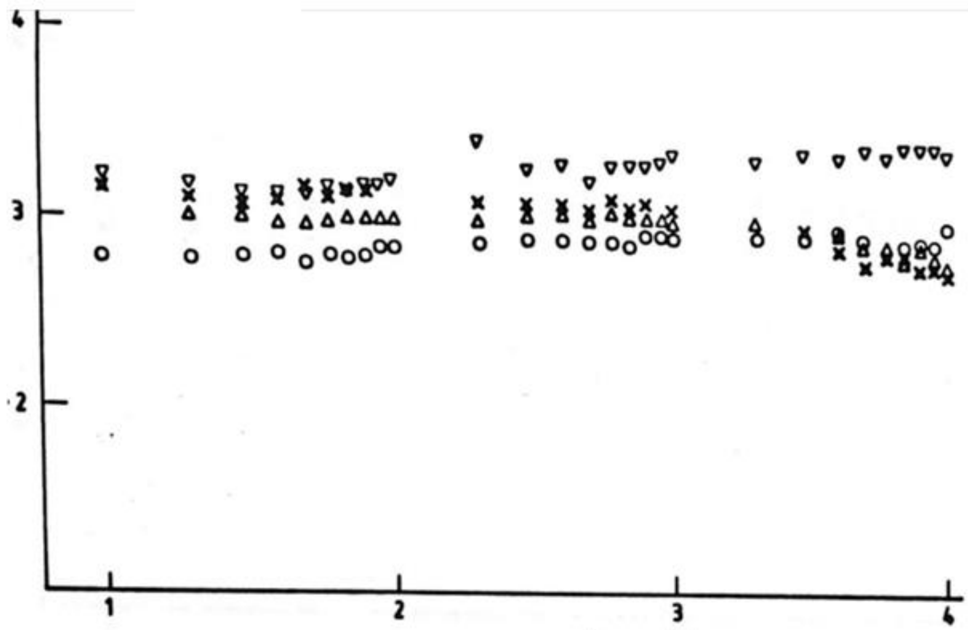


Fig. (9) Apparent compressibility function B as a function of time at constant $I_2{}' = 250\ (MN/m^2)^2$ $varying\ I_1 = 8.66$ (◯), 12.247 (Δ), 17.32($X$), 21.213(▽), $MN/m^2$

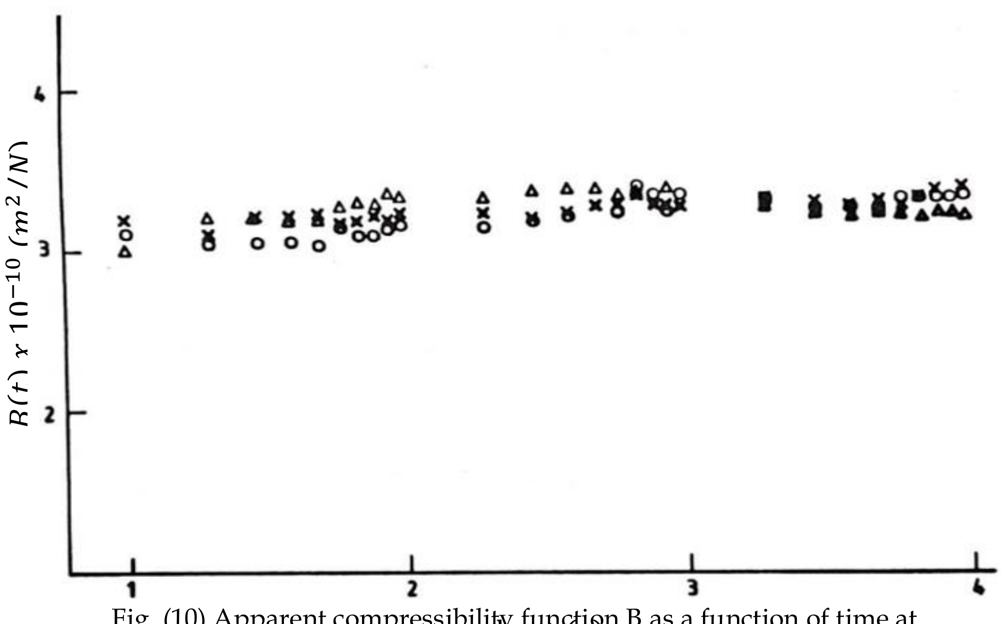


Fig. (10) Apparent compressibility function B as a function of time at constant $I_2{}' = 300\ (MN/m^2)^2$ $varying\ I_1 = 12.247$ (◯), 21.213($X$), 30.00(Δ), $MN/m^2$

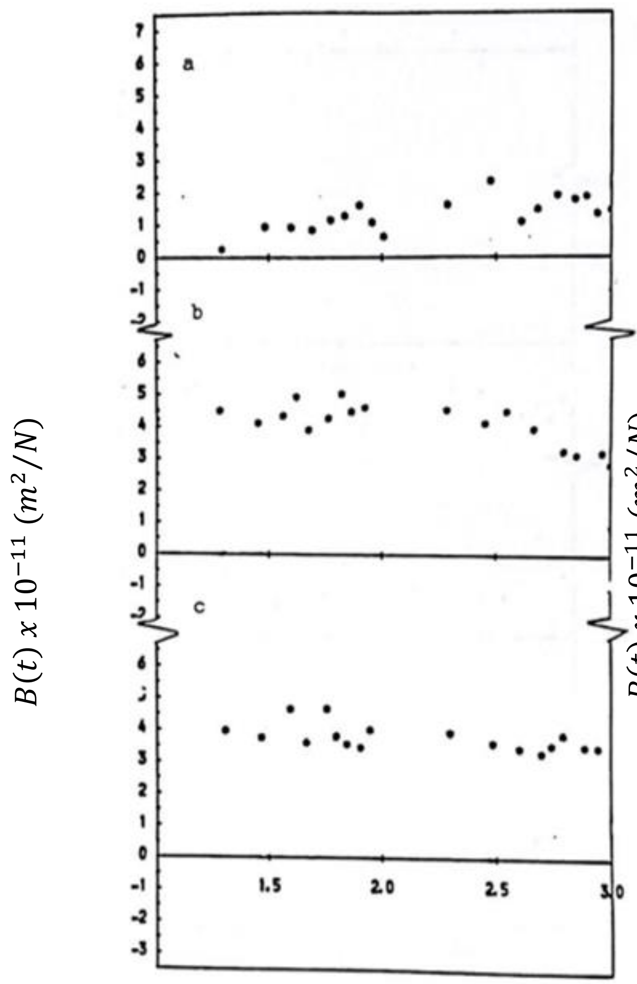


Fig. (11) The difference between creep and recovery Apparent compressibility functions $B_c$ and $B_r$ as a function of time at constant $I_1 = 27.32, 30.00, 34.467\ MN/m^2$, and varying $I_2{}' = 250\ (a), 300\ (b), 400\ (c),\ (MN/m^2)^2$

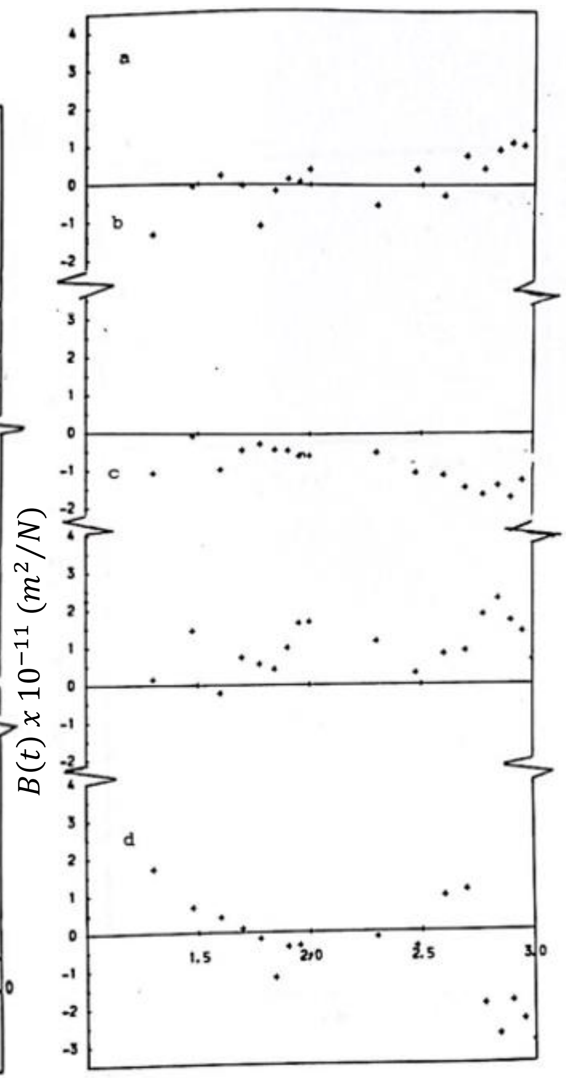


Fig. (12) The difference between creep and recovery Apparent compressibility functions $B_c$ and $B_r$ as a function of time at constant $I_1 = 12.247\ MN/m^2$ and varying $I_2{}' = 50\ (a), 100\ (b), 150\ (c), 200\ (d)\ (MN/m^2)^2$

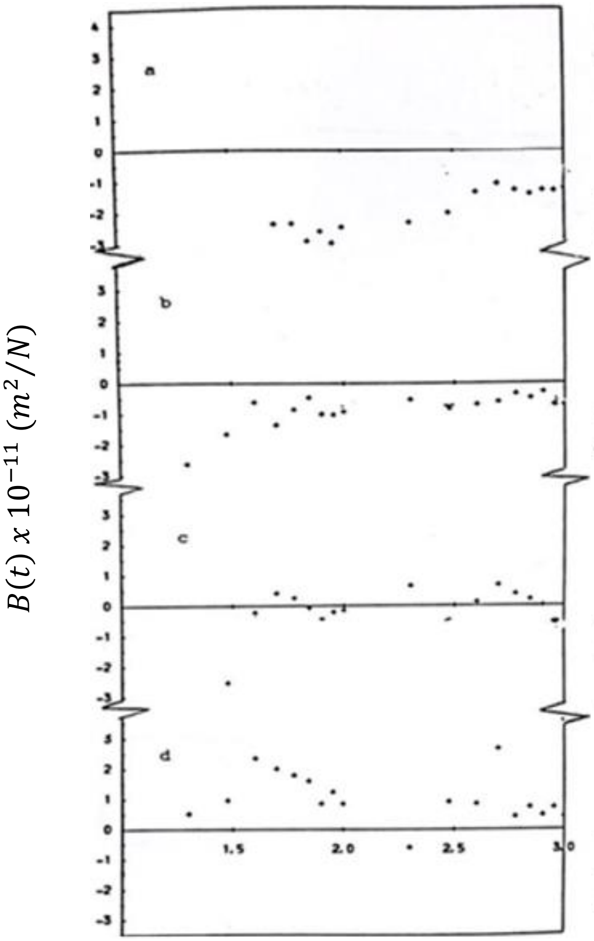


Fig. (13) The difference between creep and recovery Apparent compressibility functions $B_c$ and $B_r$ as a function of time at constant $I_1 = 17.32\ MN/m^2$ and varying $I_2{}' = 100\ (a), 150\ (b), 200\ (c), 250\ (d)\ (MN/m^2)^2$

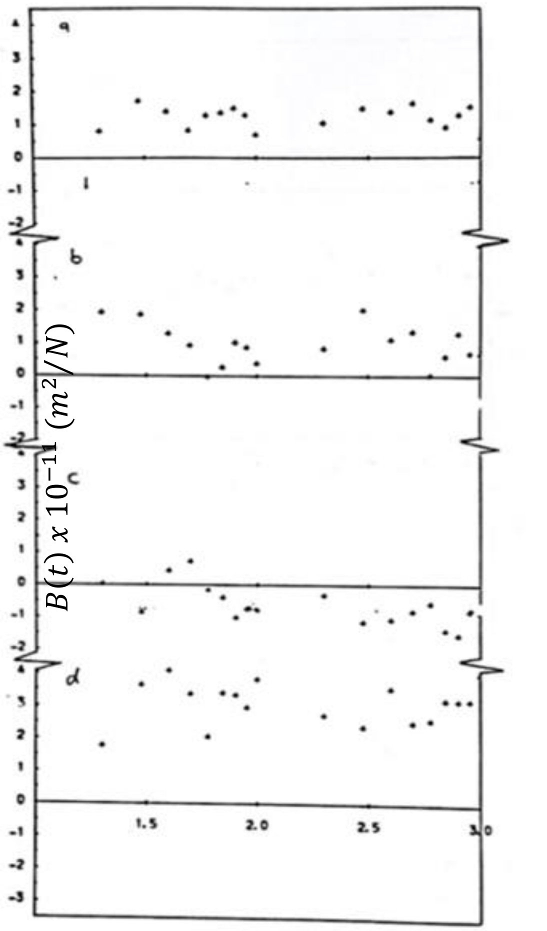


Fig. (14) The difference between creep and recovery Apparent compressibility functions $B_c$ and $B_r$ as a function of time at constant $I_1 = 21.213\ MN/m^2$ and varying $I_2{}' = 150\ (a), 200\ (b), 250\ (c), 300\ (d)\ (MN/m^2)^2$

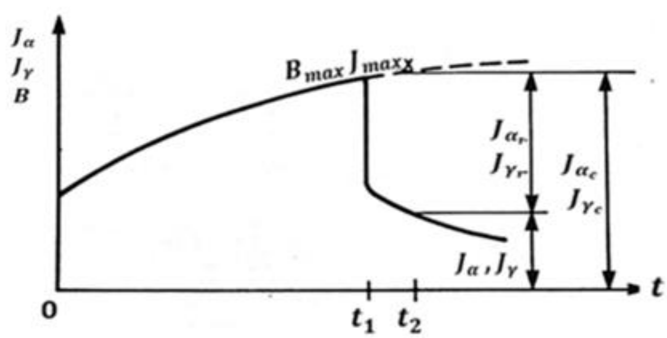


Fig. (15) Shear Compliance and Compressibility Function from tensile, lateral and shear strain

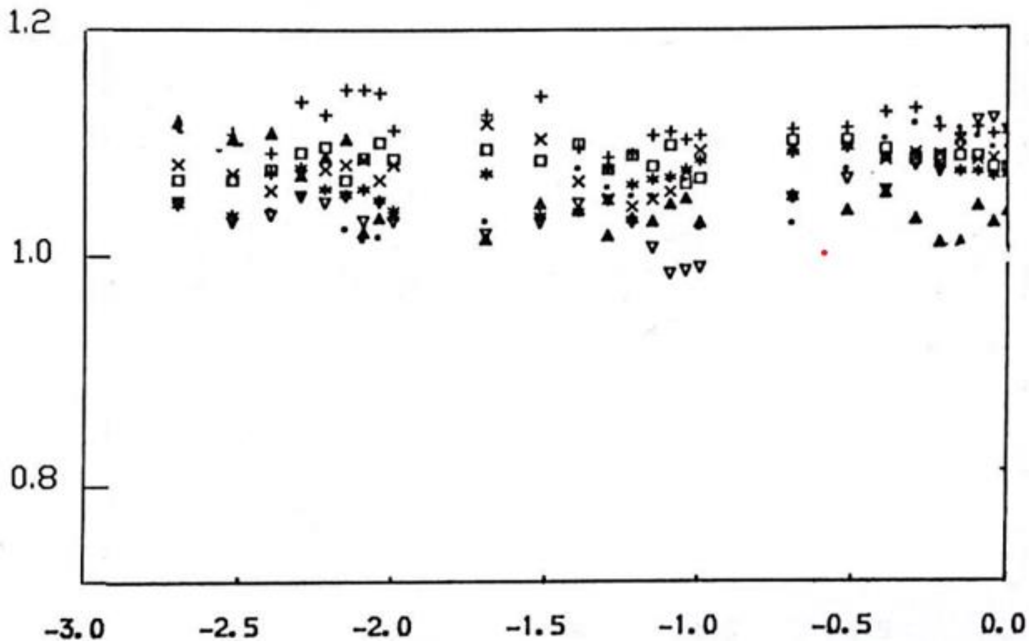


Fig. (16) Apparent compressibility function Fractional recovery $F_B$ as a function of reduced $t_R$ time at constant $I_1 = 5.477MN/m^2$ and varying $I_2{}' = 25(+), 50\ (*), 100\ (\nabla), 150\ (X), 200\ (\blacktriangle)$, $250\ (\square)\ (MN/m^2\ )^2$.

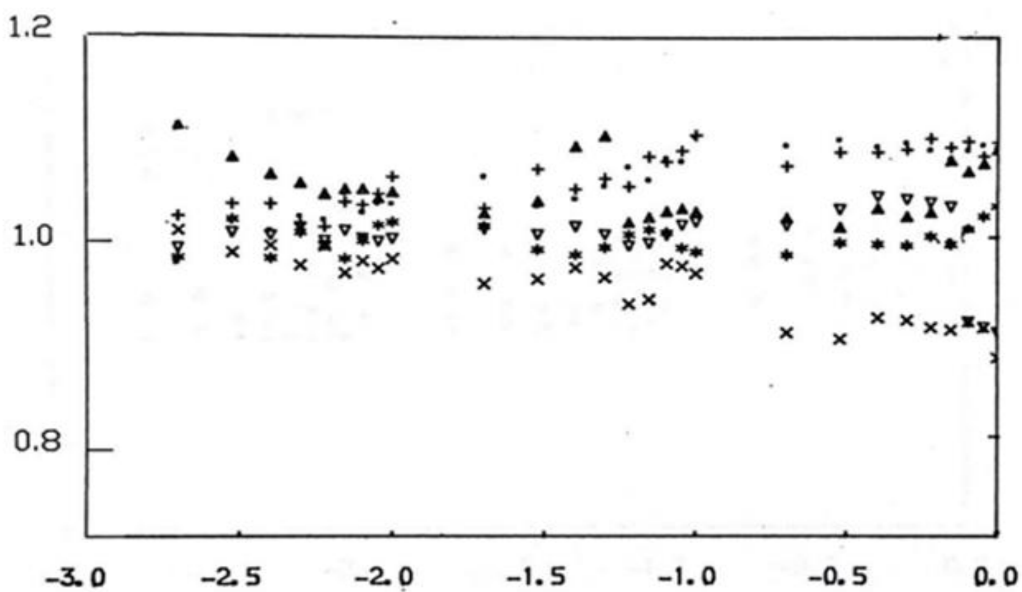


Fig. (17) Apparent compressibility function Fractional recovery $F_B$ as a function of reduced $t_R$time at constant $I_1 = 12.247MN/m^2$ and varying $I_2{}' = 50(+), 100\ (*), 150\ (\nabla), 200\ (X), 250\ (\blacktriangle)$, $300\ (\cdot)\ (MN/m^2\ )^2$

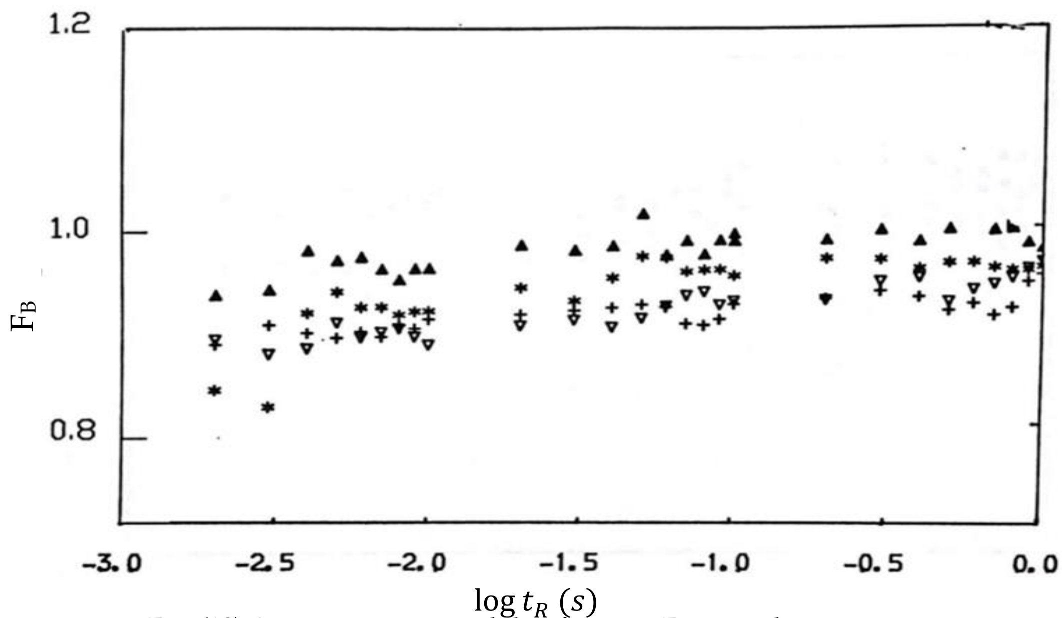


Fig. (18) Apparent compressibility function Fractional recovery $F_B$ as a function of reduced $t_R$time at constant $I_1 = 17.32 MN/m^2$ and varying $I_2{}' = 100(+), 150\ (*), 200\ (\nabla), 250\ (\blacktriangle), (MN/m^2\ )^2$

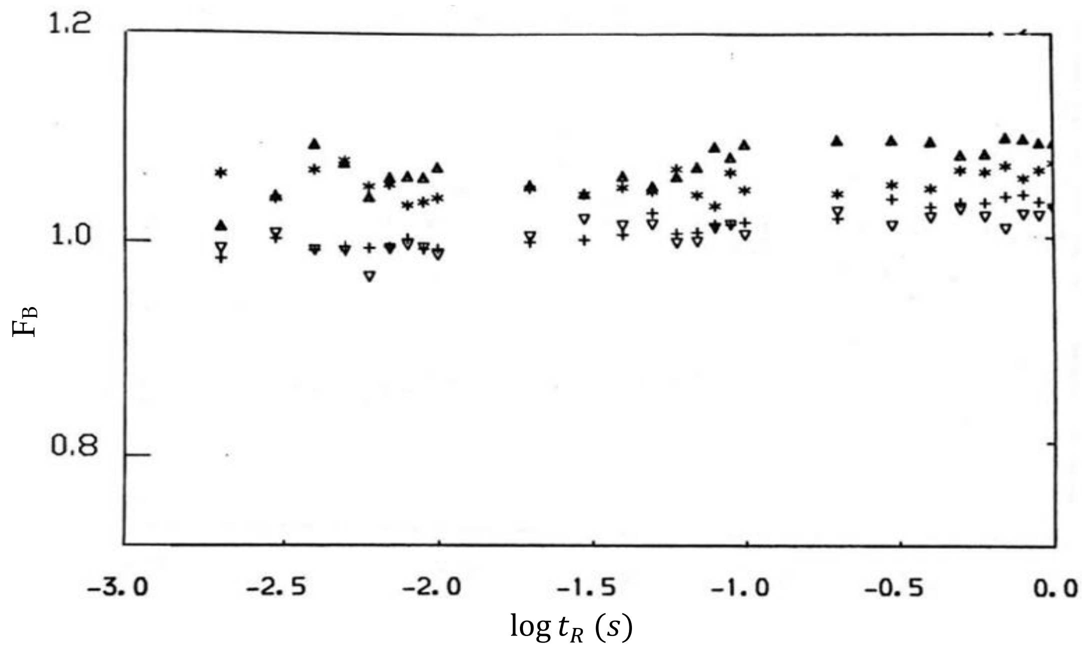


Fig. (19) Apparent compressibility function Fractional recovery $F_B$ as a function of reduced $t_R$time at constant $I_1 = 21.213 MN/m^2$ and varying $I_2{}' = 150(+), 200\ (*), 250\ (\nabla), 300\ (\blacktriangle), (MN/m^2\ )^2$

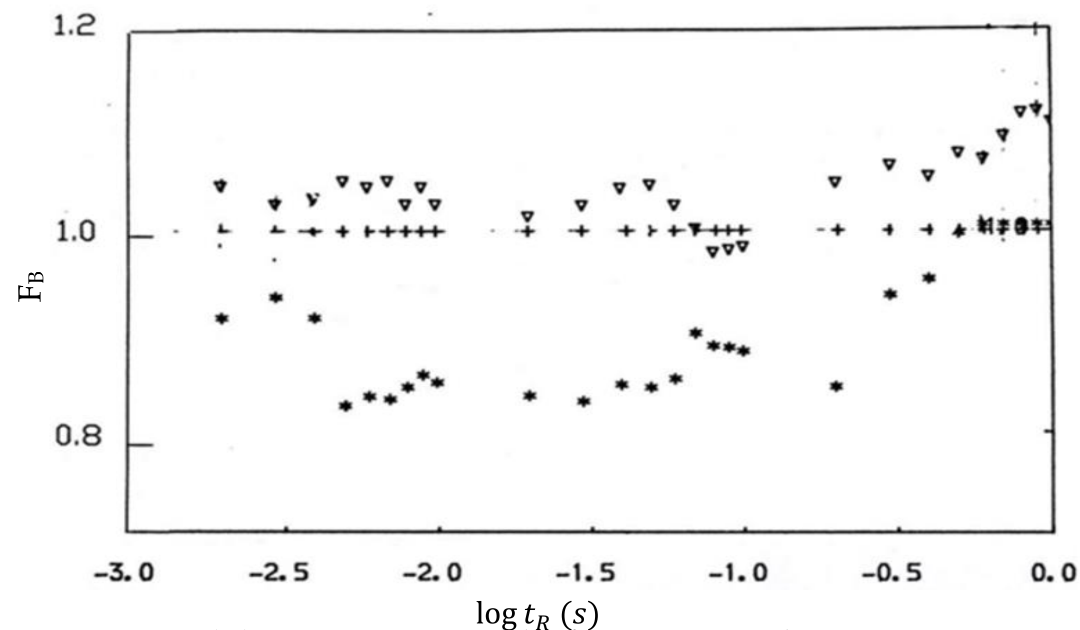


Fig. (20) Apparent compressibility function Fractional recovery $F_B$ as a function of reduced $t_R$ time at constant $I_2{}' = 25\ (MN/m^2\ )^2$ and varying $I_1 = 5.477\ (*), 8.66\ (\nabla), (MN/m^2)$

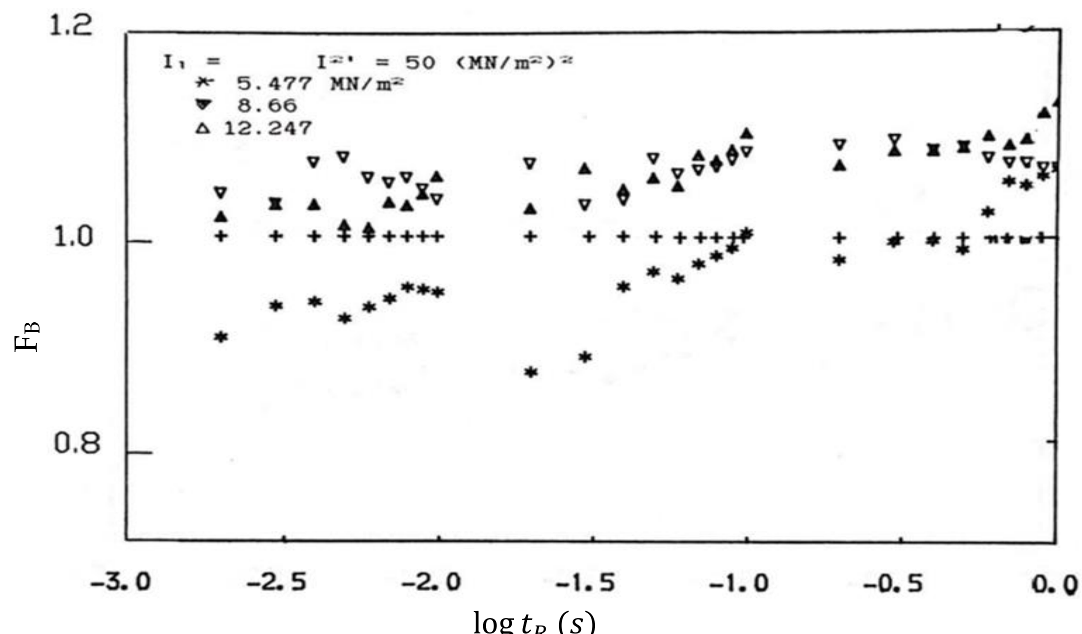


Fig. (21) Apparent compressibility function Fractional recovery $F_B$ as a function of reduced $t_R$ time at constant $I_2{}' = 50\ (MN/m^2\ )^2$ and varying $I_1 = 5.477\ (*)\ , 8.66\ (\nabla), 12.247\ (\blacktriangle), (MN/m^2)$

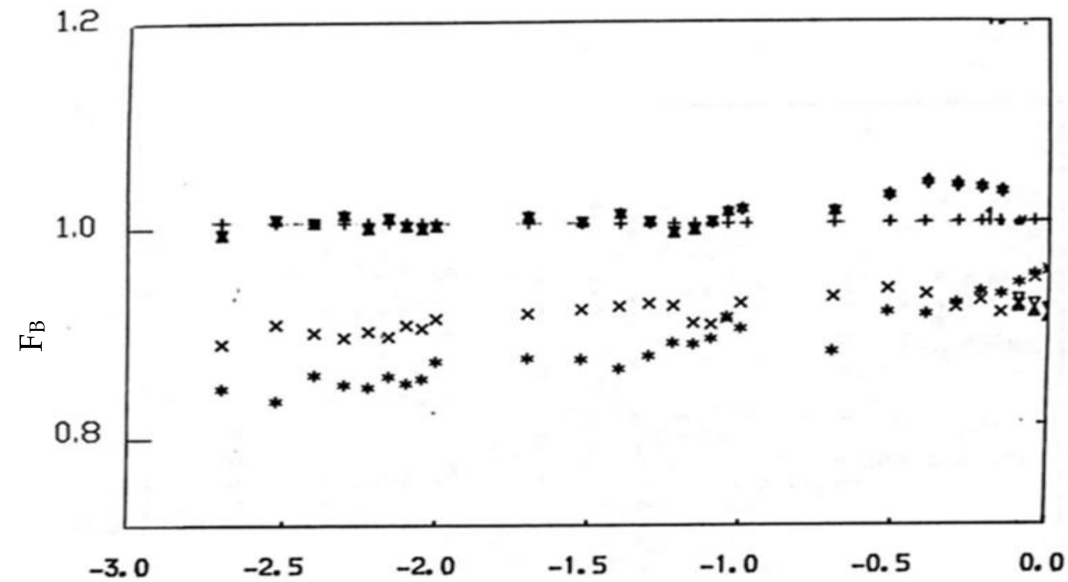


$\log t_R\ (s)$

Fig. (22) Apparent compressibility function Fractional recovery $F_B$ as a function of reduced $t_R$ time at constant $I_2{}' = 100\ (MN/m^2\ )^2$ and varying $I_1 = 5.477\ (*), 8.66\ (\nabla), 12.247\ (\blacktriangle), 17.32\ (X)$, $(MN/m^2)$

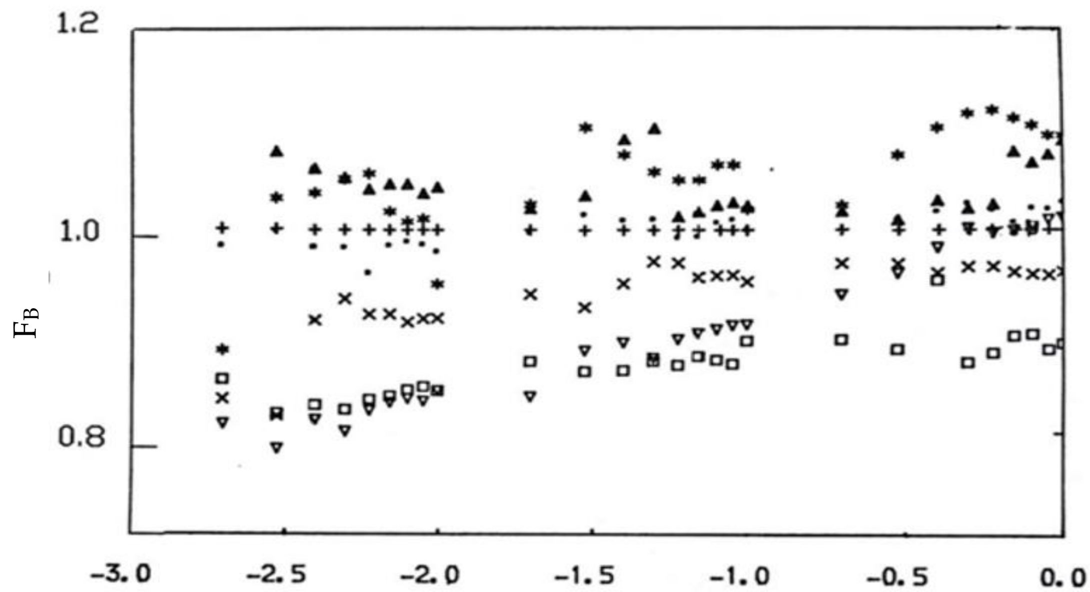


$\log t_R\ (s)$

Fig. (23) Apparent compressibility function Fractional recovery $F_B$ as a function of reduced $t_R$ time at constant $I_2{}' = 200\ (MN/m^2\ )^2$ and varying $I_1 = 5.477(*), 8.66\ (\blacktriangle), 12.247\ (\nabla),\ 17.32\ (X)$, $21.213\ (\cdot), 24.495\ (\square), (MN/m^2)$

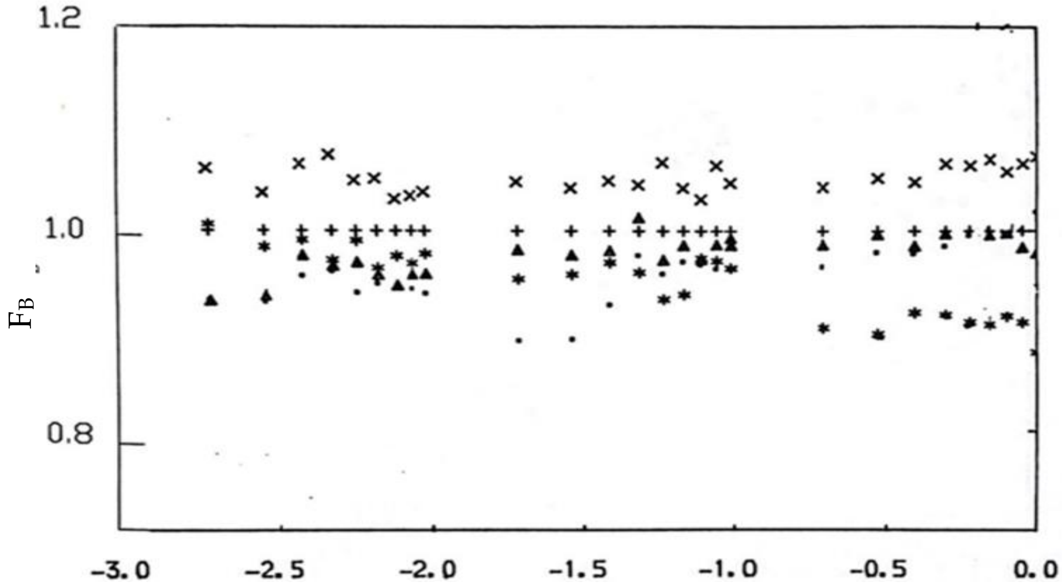


$\log t_R\ (s)$

Fig. (24) Apparent compressibility function Fractional recovery $F_B$ as a function of reduced $t_R$ time at constant $I_2' = 250\ (MN/m^2)^2$ and varying $I_1 = 8.66\ (*), 12.247\ (\blacktriangle),\ 21.213\ (X), 30.00\ (\cdot)$, $(MN/m^2)$

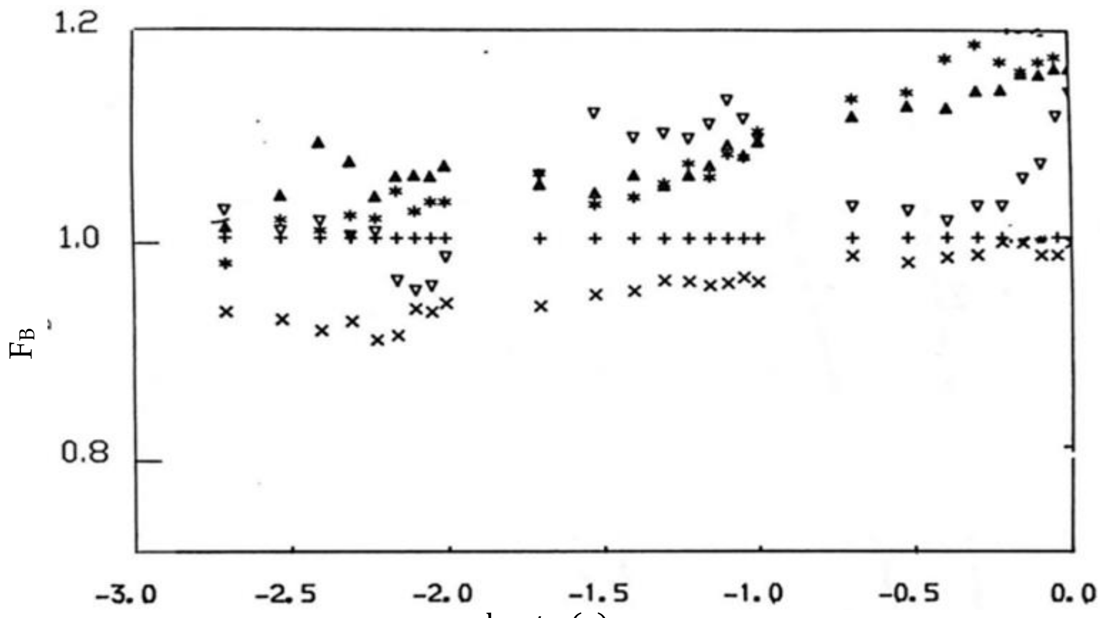


$\log t_R\ (s)$

Fig. (25) Apparent compressibility function Fractional recovery $F_B$ as a function of reduced $t_R$ time at constant $I_2' = 300\ (MN/m^2)^2$ and varying $I_1 = 5.477\ (*), 12.247\ (\blacktriangle), 21.213\ (X), 24.5\ (\nabla)$, $(MN/m^2)$.

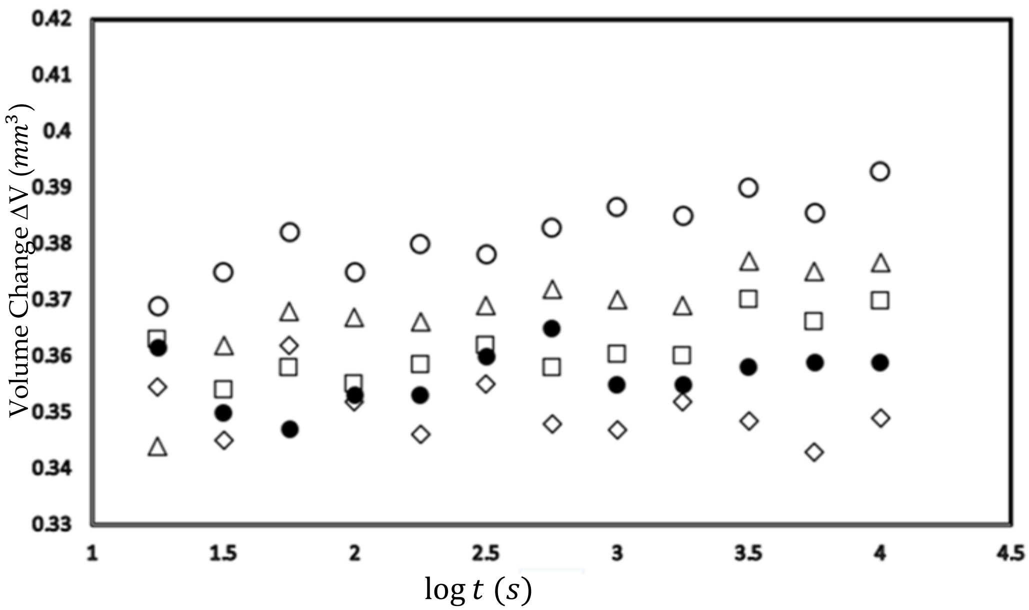


Fig. (26) Volume change ΔB as a function of time at Constant $I_1 = 12.247\ MN/m^2\ varying\ I_2{}' = 50$ ( ◊ ) 100 (●), 150 (□), 200 (Δ), 250 (○) $(MN/m^2)^2$

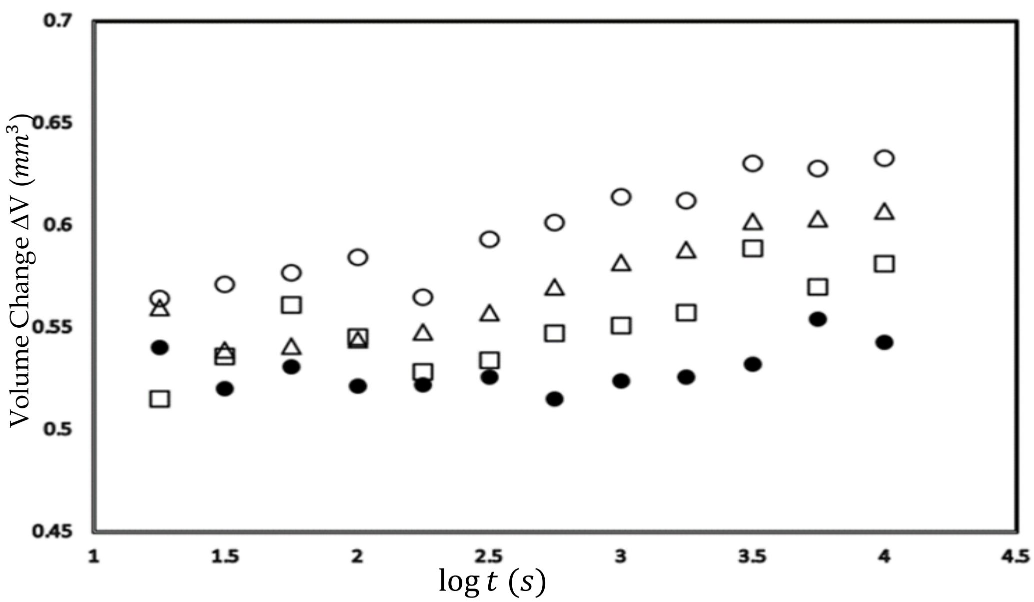


Fig. (27) Volume change ΔB as a function of time at Constant $I_1 = 17.23\ MN/m^2\ varying\ I_2{}' = 100$ (●), 150 (□), 200 (Δ), 250 (○) $(MN/m^2)^2$